Geophysical Journal International

Geophys. J. Int. (2014) **199,** 1367–1371
GJI Seismology

doi: 10.1093/gji/ggu313

EXPRESS LETTER

On the Marchenko equation for multicomponent single-sided reflection data

Kees Wapenaar and Evert Slob

Department of Geoscience and Engineering, Delft University of Technology, P.O. Box 5048, 2600 *GA Delft, the Netherlands.*
E-mail: c.p.a.wapenaar@tudelft.nl

Accepted 2014 August 11. Received 2014 August 4; in original form 2014 June 13

SUMMARY

Recent work on the Marchenko equation has shown that the scalar 3-D Green's function for a virtual source in the subsurface can be retrieved from the single-sided reflection response at the surface and an estimate of the direct arrival. Here, we discuss the first steps towards extending this result to multicomponent data. After introducing a unified multicomponent 3-D Green's function representation, we analyse its 1-D version for elastodynamic waves in more detail. It follows that the main additional requirement is that the multicomponent direct arrival, needed to initiate the iterative solution of the Marchenko equation, includes the forward-scattered field. Under this and other conditions, the multicomponent Green's function can be retrieved from single-sided reflection data, and this is demonstrated with a 1-D numerical example.

Key words: Interferometry; Controlled source seismology; Wave scattering and diffraction.

1 INTRODUCTION

Building on pioneering work by Rose (2001, 2002) on acoustic single-sided autofocusing, Broggini & Snieder (2012) showed that the Green's function for a source inside an unknown 1-D medium can be retrieved from the single-sided reflection response at the surface of that medium. Hence, like in seismic interferometry (Campillo & Paul 2003; Schuster *et al.* 2004; Curtis *et al.* 2006), a virtual source can be created inside an unknown 1-D medium, but, unlike in seismic interferometry, without needing a physical receiver at the position of the virtual source and without needing omnidirectional illumination of the medium. Using heuristic arguments, we showed that the approach of Broggini & Snieder (2012) can be extended to 3-D media (Wapenaar *et al.* 2012). Later we presented a more formal derivation by extending the 1-D Marchenko equation, underlying the work of Rose (2001, 2002) and Broggini & Snieder (2012), to a 3-D Marchenko equation (Wapenaar *et al.* 2014a). This 3-D approach to Green's function retrieval requires, apart from the reflection data at the surface, an estimate of the direct arrivals between the virtual source inside the medium and the receivers at the surface. A smooth subsurface model is usually sufficient to model these direct arrivals. The information needed to predict the multiple reflections in the 3-D Green's function comes entirely from the reflection data.

Both the 1- and 3-D approaches to retrieving the Green's function from single-sided reflection data have to date been derived for scalar waves only. These methods rely on a specific causality condition, namely, that in the time domain the coda of the so-called focusing function can be completely separated from the Green's function. This condition is strictly obeyed for 1-D scalar waves. For 3-D scalar waves the condition holds in layered media with moderately curved interfaces, assuming finite horizontal source–receiver offsets (Wapenaar *et al.* 2014a); in more complex media and/or at large offsets the condition may be violated. For 1- and 3-D vectorial waves, it has not yet been investigated to what extent the causality condition holds and how one can cope with situations in which the condition is violated. This is the main reason why the Marchenko equation has not yet been modified for multicomponent single-sided reflection data.

This paper discusses initial steps in this direction. Da Costa *et al.* (2014) pursue an independent approach. First, a unified 3-D single-sided representation is presented which expresses the multicomponent Green's function in terms of the multicomponent reflection response and a multicomponent version of the focusing function. Next, we focus on the 1-D version of this representation and analyse the causality condition for the situation of elastodynamic wavefields. Based on this analysis we propose a 1-D Marchenko equation for single-sided elastodynamic reflection data and show how it can be used for elastodynamic Green's function retrieval. We discuss its limitations and briefly indicate how the scheme can be extended to the 3-D situation.

Note that our proposal is essentially different from previous work by Budreck & Rose (1990), who use the Newton–Marchenko equation for 3-D inverse scattering in elastic media. The method of Budreck & Rose (1990) requires that the medium is illuminated from all directions and that the response is also measured in all directions (which involves reflection as well as transmission responses). In contrast, the method proposed here requires a reflection response, measured at one side of the medium only, and a specific initial estimate of the multicomponent focusing function.

2 A UNIFIED GREEN'S FUNCTION REPRESENTATION

Consider a 3-D inhomogeneous lossless medium below a horizontal boundary $\partial\mathbb{D}_0$; the half-space above this boundary is homogeneous (Fig. 1a). In the space-time $(\mathbf{x}, t)$ domain, an $N \times 1$ wavefield vector $\mathbf{u}^+(\mathbf{x}, t)$, containing the N components of a flux-normalized decomposed downgoing wavefield, is incident to the medium from above. In our unified treatment, the wavefield can be an electromagnetic or an elastodynamic wavefield (or a coupled field in a piezoelectric or poroelastic medium). For example, in the case of a 3-D elastodynamic wavefield, the components of $\mathbf{u}^+(\mathbf{x}, t)$ represent the downgoing compressional wave and the two types of downgoing shear waves. The response of the medium to $\mathbf{u}^+(\mathbf{x}, t)$ is denoted in the upper half-space above $\partial\mathbb{D}_0$ as $\mathbf{u}^-(\mathbf{x}, t)$, which is a wavefield vector containing N decomposed upgoing wavefield components. At $\partial\mathbb{D}_0$ these wave vectors are related via

$$\mathbf{u}^-(\mathbf{x}_0, t) = \int_{\partial\mathbb{D}_0} \mathrm{d}\mathbf{x}_0' \int_{-\infty}^{t} \mathbf{R}(\mathbf{x}_0, \mathbf{x}_0', t - t')\mathbf{u}^+(\mathbf{x}_0', t')\,\mathrm{d}t', \tag{1}$$

where $\mathbf{R}(\mathbf{x}_0, \mathbf{x}_0', t)$ is the $N \times N$ reflection response matrix of the inhomogeneous medium below $\partial\mathbb{D}_0$. The subscript 0 in $\mathbf{x}_0$ and $\mathbf{x}_0'$ denotes that these coordinate vectors are defined at $\partial\mathbb{D}_0$, hence $\mathbf{x}_0 = (\mathbf{x}_\mathrm{H}, z_0)$ and $\mathbf{x}_0' = (\mathbf{x}_\mathrm{H}', z_0)$, where z_0 denotes the depth of $\partial\mathbb{D}_0$, and $\mathbf{x}_\mathrm{H} = (x, y)$ represents the horizontal coordinate vector. Each column in $\mathbf{R}(\mathbf{x}_0, \mathbf{x}_0', t)$ contains N upgoing wavefield components at $\mathbf{x}_0$, in response to a specific type of source for downgoing waves at $\mathbf{x}_0'$; the N columns correspond to N source types (e.g. one source for downgoing compressional waves and two sources for downgoing shear waves in the elastodynamic case).

At an arbitrary chosen depth z_i (below z_0), we define a second boundary $\partial\mathbb{D}_i$ and we denote coordinate vectors at this boundary as $\mathbf{x}_i = (\mathbf{x}_\mathrm{H}, z_i)$. At $\partial\mathbb{D}_i$, the response to $\mathbf{u}^+(\mathbf{x}_0, t)$ is denoted as $\mathbf{u}^+(\mathbf{x}_i, t)$ (for the downgoing part) and $\mathbf{u}^-(\mathbf{x}_i, t)$ (for the upgoing part). Analogous to eq. (1), we introduce $N \times N$ Green's matrices via

$$\mathbf{u}^\pm(\mathbf{x}_i, t) = \int_{\partial\mathbb{D}_0} \mathrm{d}\mathbf{x}_0' \int_{-\infty}^{t} \mathbf{G}^{\pm,+}(\mathbf{x}_i, \mathbf{x}_0', t - t')\mathbf{u}^+(\mathbf{x}_0', t')\,\mathrm{d}t'. \tag{2}$$

Here the second superscript of the Green's matrix (+) denotes the downward propagation direction at the Green's source at $\mathbf{x}_0'$, whereas the first superscript (±) refers to the propagation direction at the observation point $\mathbf{x}_i$ (Fig. 1a). Note that our definition of the Green's matrix is different from that in seismological textbooks. In the Supporting Information we discuss their mutual relation (eqs A36–A51).

Our goal is to find a representation for the Green's matrices $\mathbf{G}^{\pm,+}(\mathbf{x}_i, \mathbf{x}_0', t)$ in terms of the reflection response matrix $\mathbf{R}(\mathbf{x}_0, \mathbf{x}_0', t)$. To this end, we first introduce a reference configuration, which is identical to the actual medium above $\partial\mathbb{D}_i$ but reflection-free below this boundary (Fig. 1b). An $N \times N$ focusing wavefield matrix $\mathbf{F}_1^+(\mathbf{x}, \mathbf{x}_i', t)$ is incident to this reference configuration from above. This field is shaped (as a function of $\mathbf{x}$ and t) such that it focuses at focal point $\mathbf{x}_i'$ at boundary $\partial\mathbb{D}_i$ at $t = 0$ [i.e. each column of $\mathbf{F}_1^+(\mathbf{x}, \mathbf{x}_i', t)$ focuses onto one specific wave type at the focal point]. Hence, the response to $\mathbf{F}_1^+(\mathbf{x}, \mathbf{x}_i', t)$ at $\partial\mathbb{D}_i$ is defined as $\mathbf{F}_1^+(\mathbf{x}_i, \mathbf{x}_i', t) = \mathbf{I}\delta(\mathbf{x}_\mathrm{H} - \mathbf{x}_\mathrm{H}')\delta(t)$. The delta functions should be interpreted in a band-limited sense (evanescent waves are not included), and $\mathbf{I}$ is an $N \times N$ identity matrix. The focusing matrix at $\partial\mathbb{D}_0$ and its response at $\partial\mathbb{D}_i$ are related, similar to eqs (1) and (2), via

$$\begin{aligned}\mathbf{F}_1^+(\mathbf{x}_i, \mathbf{x}_i', t) &= \mathbf{I}\delta(\mathbf{x}_\mathrm{H} - \mathbf{x}_\mathrm{H}')\delta(t)\\ &= \int_{\partial\mathbb{D}_0} \mathrm{d}\mathbf{x}_0'' \int_{-\infty}^{t} \mathbf{T}(\mathbf{x}_i, \mathbf{x}_0'', t - t')\mathbf{F}_1^+(\mathbf{x}_0'', \mathbf{x}_i', t')\,\mathrm{d}t'.\end{aligned} \tag{3}$$

Here $\mathbf{T}(\mathbf{x}_i, \mathbf{x}_0'', t)$ is the $N \times N$ transmission response matrix of the reference configuration between $\partial\mathbb{D}_0$ and $\partial\mathbb{D}_i$. According to eq. (3), the focusing matrix $\mathbf{F}_1^+(\mathbf{x}_0'', \mathbf{x}_i', t)$ is the inverse of this transmission response matrix. For a comparison of this focusing condition with that in time-reversed acoustics, see Wapenaar *et al.* (2014b). In the upper half-space, the response to $\mathbf{F}_1^+(\mathbf{x}, \mathbf{x}_i', t)$ is denoted as $\mathbf{F}_1^-(\mathbf{x}, \mathbf{x}_i', t)$. Because the reference configuration is reflection-free below $\partial\mathbb{D}_i$ there is no upgoing field at $\partial\mathbb{D}_i$, hence $\mathbf{F}_1^-(\mathbf{x}_i, \mathbf{x}_i', t) = \mathbf{O}$, where $\mathbf{O}$ is an $N \times N$ zero matrix.

A unified representation for the Green's matrices is obtained by substituting all quantities introduced into reciprocity theorems for downgoing and upgoing wavefields. The procedure is similar to that for the scalar situation (Slob *et al.* 2014; Wapenaar *et al.* 2014a). The main difference is that, because we deal with matrices, the order of multiplications matters. The details of the derivation can be found in the Supporting Information. The resulting expressions are

$$\begin{aligned}&\mathbf{G}^{-,+}(\mathbf{x}_0'', \mathbf{x}_i', t) + \mathbf{F}_1^-(\mathbf{x}_0'', \mathbf{x}_i', t)\\ &\quad= \int_{\partial\mathbb{D}_0} \mathrm{d}\mathbf{x}_0 \int_{-\infty}^{t} \mathbf{R}(\mathbf{x}_0'', \mathbf{x}_0, t - t')\mathbf{F}_1^+(\mathbf{x}_0, \mathbf{x}_i', t')\,\mathrm{d}t'\end{aligned} \tag{4}$$

and

$$\begin{aligned}&\mathbf{G}^{-,-}(\mathbf{x}_0'', \mathbf{x}_i', t) + \mathbf{F}_1^+(\mathbf{x}_0'', \mathbf{x}_i', -t)\\ &\quad= \int_{\partial\mathbb{D}_0} \mathrm{d}\mathbf{x}_0 \int_{-\infty}^{t} \mathbf{R}(\mathbf{x}_0'', \mathbf{x}_0, t - t')\mathbf{F}_1^-(\mathbf{x}_0, \mathbf{x}_i', -t')\,\mathrm{d}t',\end{aligned} \tag{5}$$

respectively. Note that the Green's matrices in these representations are the reciprocals of those in eq. (2), with $\mathbf{G}^{-,+}(\mathbf{x}_0'', \mathbf{x}_i', t) = \{\mathbf{G}^{-,+}(\mathbf{x}_i', \mathbf{x}_0'', t)\}^t$ and $\mathbf{G}^{-,-}(\mathbf{x}_0'', \mathbf{x}_i', t) = -\{\mathbf{G}^{+,+}(\mathbf{x}_i', \mathbf{x}_0'', t)\}^t$ (superscript t denotes transposition). In these representations, the Green's

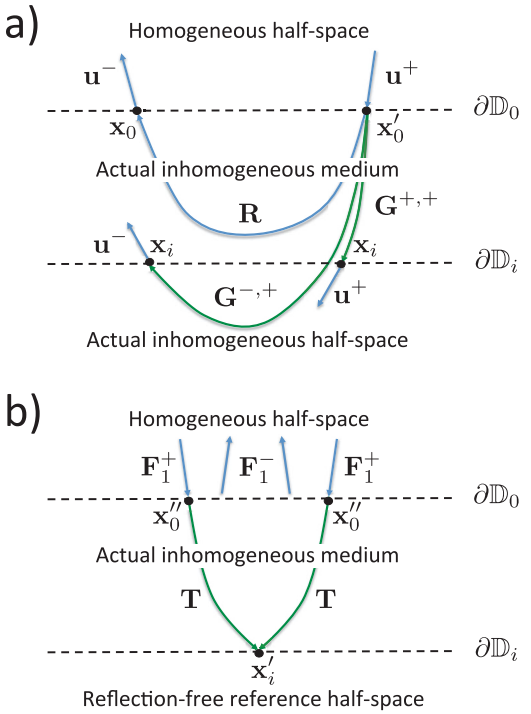

Figure 1. (a) Reflection response and Green's functions in actual medium (eqs 1 and 2). (b) Focusing functions and transmission response in reference configuration (eq. 3).

wavefields originate from a virtual source at $\mathbf{x}_i'$, which coincides with the focal point of the focusing function [each column of $\mathbf{G}^{-,\pm}(\mathbf{x}_0'', \mathbf{x}_i', t)$ corresponds to one specific wave type radiated by the virtual source]. In eq. (4), the virtual source radiates downwards, denoted by the second superscript (+) of the Green's function; similarly, in eq. (5) it radiates upwards, also denoted by the second superscript (−). In both representations the first superscript of the Green's function (−) refers to the upward propagation direction at the observation point $\mathbf{x}_0''$ at the surface $\partial\mathbb{D}_0$. Representations (4) and (5) form a unified basis for retrieving the multicomponent Green's functions from the single-sided multicomponent reflection response and the multicomponent focusing functions. The main question is how to retrieve the multicomponent focusing functions from the reflection response. Once the focusing functions are known, the Green's functions follow immediately and can be used for multicomponent imaging. In the following, we analyse a 1-D version of eqs (4) and (5) to gain insight in the possibilities and limitations of retrieving the focusing functions from the reflection response.

3 ANALYSIS OF THE 1-D REPRESENTATION

From here onwards we assume that the medium is horizontally layered. Moreover, we consider elastodynamic propagation in the (x, z)-plane, assuming the wavefields are constant in the y-direction. By applying a plane wave decomposition, the x-coordinate is replaced by the horizontal rayparameter p. In the rayparameter intercept-time (p, τ) domain, eqs (4) and (5) become

$$\mathbf{G}^{-,+}(p, z_0, z_i, \tau) + \mathbf{F}_1^{-}(p, z_0, z_i, \tau) = \int_{-\infty}^{\tau} \mathbf{R}(p, z_0, \tau - \tau')\mathbf{F}_1^{+}(p, z_0, z_i, \tau')\,\mathrm{d}\tau' \tag{6}$$

and

$$\mathbf{G}^{-,-}(p, z_0, z_i, \tau) + \mathbf{F}_1^{+}(-p, z_0, z_i, -\tau) = \int_{-\infty}^{\tau} \mathbf{R}(p, z_0, \tau - \tau')\,\mathbf{F}_1^{-}(-p, z_0, z_i, -\tau')\,\mathrm{d}\tau', \tag{7}$$

respectively (see the Supporting Information for a derivation). The matrices are 2×2 matrices, for example,

$$\mathbf{G}^{-,\pm} = \begin{pmatrix} G_{P,P}^{-,\pm} & G_{P,S}^{-,\pm} \\ G_{S,P}^{-,\pm} & G_{S,S}^{-,\pm} \end{pmatrix}, \quad \mathbf{F}_1^{\pm} = \begin{pmatrix} f_{P,P}^{\pm} & f_{P,S}^{\pm} \\ f_{S,P}^{\pm} & f_{S,S}^{\pm} \end{pmatrix}. \tag{8}$$

The subscripts P and S stand for compressional and shear waves, respectively. Note that in eqs (6) and (7), the left columns in these two matrices can be considered independent from the right columns.

First, we analyse $\mathbf{G}^{-,\pm}$ and $\mathbf{F}_1^{\pm}$ by direct modelling in the horizontally layered medium of Fig. 2, with $z_i = 1000$ m. $\mathbf{F}_1^{+}$ is obtained as the inverse of the modelled transmission response $\mathbf{T}$ of the reference configuration, see eq. (3) and Fig. 1(b); $\mathbf{F}_1^{-}$ is the reflection response to $\mathbf{F}_1^{+}$ in the reference configuration. For normal incidence ($p = 0$) no conversion takes place, hence, the PP elements of $\mathbf{G}^{-,\pm}$ and $\mathbf{F}_1^{\pm}$ are the same as in the acoustic case. They are shown in Fig. 3, convolved with a zero-phase wavelet with a central frequency of 50 Hz. Here τ_{PP}^{d} indicates the time of the onset of the direct arrival of $G_{P,P}^{-,-}$. Figs 3(a) and (b) represent the left-hand sides of eqs (6) and (7), respectively. Note that $G_{P,P}^{-,+}$ and $f_{P,P}^{-}$ are well separated in time (Fig. 3a), whereas $G_{P,P}^{-,-}$ and the time-reversal of $f_{P,P}^{+}$ overlap each other at the direct arrival of $G_{P,P}^{-,-}$ (Fig. 3b). The overlapping events cannot be resolved from eqs (6) and (7). Therefore, in the acoustic Marchenko scheme the direct arrival is estimated separately and its inverse is taken as the initial estimate of $f_{P,P}^{+}$. The coda of $f_{P,P}^{+}$ and

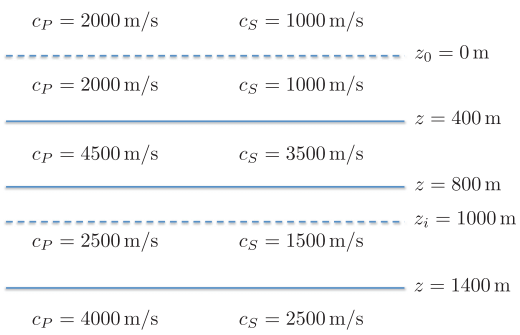

Figure 2. Horizontally layered medium (the mass density is 2000 kg m^{-3} in all layers). The dashed line at $z_i = 1000$ m denotes the depth of the virtual source.

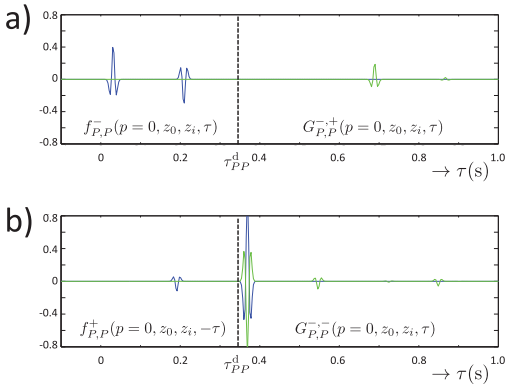

Figure 3. Directly modelled Green's functions (green) and focusing functions (blue) for normal incidence ($p = 0$).

the entire function $f_{P,P}^{-}$ are subsequently resolved from the scalar version of eqs (6) and (7) for $\tau < \tau_{PP}^{\mathrm{d}}$ (Broggini & Snieder 2012; Wapenaar *et al.* 2012; Slob *et al.* 2014).

For oblique incidence ($p = 0.0002$ s m^{-1}, corresponding to an angle of 24° for P waves in the first layer), the PP and SP elements of $\mathbf{G}^{-,\pm}$ and $\mathbf{F}_1^{\pm}$ (i.e. their left columns) are shown in Fig. 4 (the complete matrices are shown in Figs S2 and S3). Here τ_{SP}^{d} indicates the time of the onset of the first arrival of $G_{S,P}^{-,-}$ (this wave starts as an upgoing P wave at $z_i = 1000$ m, converts to an S wave at $z = 400$ m and hence arrives as an S wave at $z_0 = 0$ m). Figs 4(a) and (b) represent the left-hand side of eq. (6). Note that here the Green's functions and focusing functions are well separated in time, but, unlike in the scalar case, this separation is not guaranteed. For example, when z_i is close to an interface, the focusing functions may extend into the region of the Green's function. For now we will assume this is not the case. Figs 4(c) and (d) represent the left-hand side of eq. (7). Note that in both figures two events of the Green's function and the time-reversed focusing function overlap. In more complex media more events will overlap. The overlap is caused by the fact that different wave modes propagate with different velocities.

4 A MULTICOMPONENT SINGLE-SIDED MARCHENKO SCHEME

In the previous section we obtained $\mathbf{G}^{-,\pm}$ and $\mathbf{F}_1^{\pm}$ by direct modelling. Here we investigate how they can be resolved from eqs (6) and (7). First, note that the overlapping events in Figs 4(c) and (d) cannot be resolved from these equations. Like in the acoustic case, we define an initial estimate of the time-reversal of $\mathbf{F}_1^{+}$,

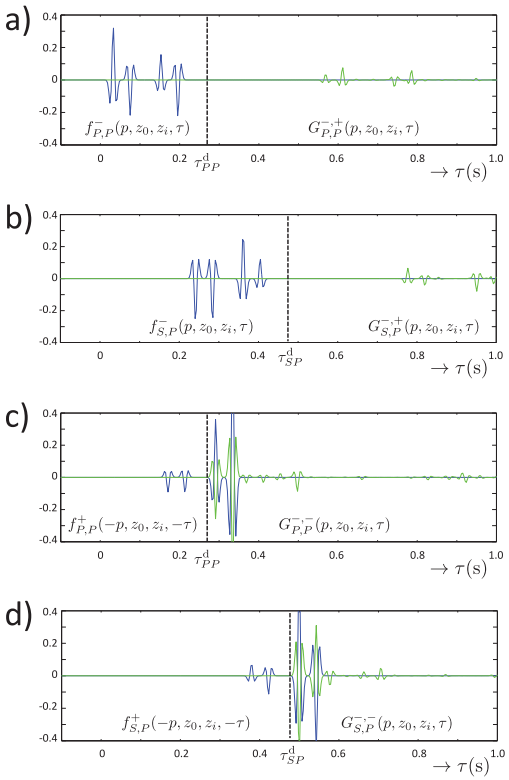

Figure 4. Directly modelled Green's functions (green) and focusing functions (blue) for oblique incidence ($p = 0.0002$ s m^{-1}).

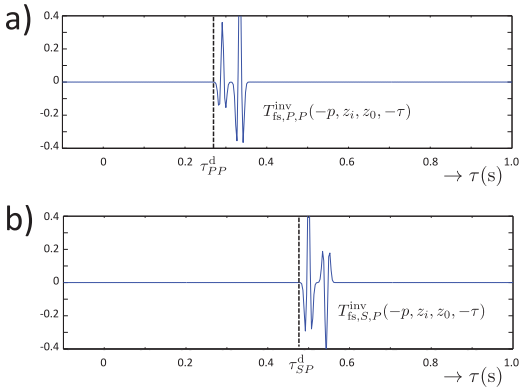

Figure 5. Inverse of the forward-scattering transmission response. This is used as the initial estimate of the focusing functions in Figs 4(c) and (d).

consisting of the events that overlap with $\mathbf{G}^{-,-}$. Recalling that $\mathbf{F}_1^+$ is the inverse of the transmission response $\mathbf{T}$ of the reference configuration (eq. 3 or A20), we define its initial estimate as the inverse of the 'forward-scattering' transmission response, that is, $\mathbf{F}_{1,0}^+(p, z_0, z_i, \tau) = \mathbf{T}_{\mathrm{fs}}^{\mathrm{inv}}(p, z_i, z_0, \tau)$. Here the 'forward-scattering' transmission response $\mathbf{T}_{\mathrm{fs}}$ is defined as the part of the transmission response which includes direct and forward converted waves but no internal multiples. Fig. 5 shows the *PP* and *SP* elements of $\mathbf{T}_{\mathrm{fs}}^{\mathrm{inv}}(-p, z_i, z_0, -\tau)$ (the complete matrix is shown in Fig. S4). These are equal to the overlapping parts of the *PP* and *SP* elements of $\mathbf{F}_1^+(-p, z_0, z_i, -\tau)$ in Figs 4(c) and (d). We used the true medium between z_0 and z_i to obtain Fig. 5. In practice an estimate of the medium will be used. We come back to this in the concluding remarks. For $\mathbf{F}_1^+(p, z_0, z_i, \tau)$ we now write

$$\mathbf{F}_1^+(p, z_0, z_i, \tau) = \mathbf{T}_{\mathrm{fs}}^{\mathrm{inv}}(p, z_i, z_0, \tau) + \mathbf{M}^+(p, z_0, z_i, \tau), \tag{9}$$

where $\mathbf{M}^+(p, z_0, z_i, \tau)$ is the coda. Our aim is now to derive a Marchenko scheme that retrieves $\mathbf{M}^+(p, z_0, z_i, \tau)$ and $\mathbf{F}_1^-(p, z_0, z_i, \tau)$ from the reflection response $\mathbf{R}(p, z_0, \tau)$, assuming the initial estimate $\mathbf{T}_{\mathrm{fs}}^{\mathrm{inv}}(p, z_i, z_0, \tau)$ is known. We define a time-window matrix $\mathbf{W}(\tau)$, according to

$$\mathbf{W}(\tau) = \begin{pmatrix} H(\tau_{PP}^{\mathrm{d}} - \tau) & H(\tau_{PS}^{\mathrm{d}} - \tau) \\ H(\tau_{SP}^{\mathrm{d}} - \tau) & H(\tau_{SS}^{\mathrm{d}} - \tau) \end{pmatrix}, \tag{10}$$

where $H(\tau)$ is the Heaviside step function. The elements of $\mathbf{W}(\tau)$ are equal to 1 left of the dashed lines at τ_{XY}^{d} in Figs 4, S2 and S3, and equal to 0 right of these dashed lines. Here τ_{XY}^{d} indicates the time of the onset of the first arrival of $G_{X,Y}^{-,-}$ (note that the first arrival of $G_{S,S}^{-,-}$ is a twice converted wave). We apply $\mathbf{W}(\tau)$ via a Hadamard matrix multiplication [i.e. $\mathbf{W}(\tau) \circ \mathbf{X}(\tau)$, which defines element-wise multiplication] to both sides of eqs (6) and (7). This removes the Green's functions from the left-hand sides. Moreover, it replaces $\mathbf{F}_1^+(-p, z_0, z_i, -\tau)$ in the left-hand side of eq. (7) by $\mathbf{M}^+(-p, z_0, z_i, -\tau)$. We thus obtain a coupled set of two Marchenko equations for the two unknowns $\mathbf{M}^+(p, z_0, z_i, \tau)$ and $\mathbf{F}_1^-(p, z_0, z_i, \tau)$. This set of equations can be solved iteratively, according to

$$\mathbf{M}_k^+(p, z_0, z_i, -\tau) = \mathbf{W}(\tau) \circ \int_{-\infty}^{\tau} \mathbf{R}^t(p, z_0, \tau - \tau') \mathbf{F}_{1,k}^-(p, z_0, z_i, -\tau')\, \mathrm{d}\tau' \tag{11}$$

[where $\mathbf{R}^t(p, z_0, \tau) = \mathbf{R}(-p, z_0, \tau)$] and

$$\mathbf{F}_{1,k+1}^-(p, z_0, z_i, \tau) = \mathbf{F}_{1,0}^-(p, z_0, z_i, \tau) + \mathbf{W}(\tau) \circ \int_{-\infty}^{\tau} \mathbf{R}(p, z_0, \tau - \tau') \mathbf{M}_k^+(p, z_0, z_i, \tau')\, \mathrm{d}\tau', \tag{12}$$

with

$$\mathbf{F}_{1,0}^-(p, z_0, z_i, \tau) = \mathbf{W}(\tau) \circ \int_{-\infty}^{\tau} \mathbf{R}(p, z_0, \tau - \tau') \mathbf{T}_{\mathrm{fs}}^{\mathrm{inv}}(p, z_i, z_0, \tau')\, \mathrm{d}\tau'. \tag{13}$$

We apply this iterative scheme for $k = 0 \cdots 3$, using the reflection response $\mathbf{R}(p, z_0, \tau)$ and the inverse of the forward-scattering transmission response, $\mathbf{T}_{\mathrm{fs}}^{\mathrm{inv}}(p, z_i, z_0, \tau)$ (Fig. 5), as input. The results for $k = 3$ are our final estimates of $\mathbf{M}^+(p, z_0, z_i, \tau)$ and $\mathbf{F}_1^-(p, z_0, z_i, \tau)$. Using eq. (9) we construct $\mathbf{F}_1^+(p, z_0, z_i, \tau)$. After repeating the procedure for the opposite rayparameter $-p$ we are able to retrieve the Green's functions $\mathbf{G}^{-,+}(p, z_0, z_i, \tau)$ and $\mathbf{G}^{-,-}(p, z_0, z_i, \tau)$ via eqs (6) and (7). Their *PP* and *SP* elements are shown in Fig. 6 (the complete matrices are shown in Figs S6 and S7). The absolute

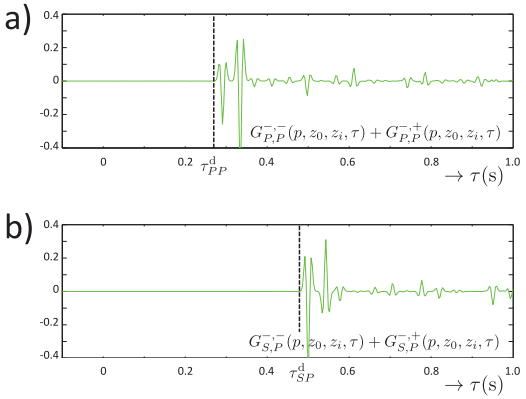

Figure 6. Retrieved Green's functions after four iterations of the Marchenko scheme.

difference with the directly modelled Green's functions in Fig. 4 is smaller than 10^{-3} (after 10 iterations the difference is smaller than 10^{-5}).

5 CONCLUDING REMARKS

The analysis in this paper shows that, at least in principle, the multicomponent Green's function for a virtual source inside a medium can be retrieved from the multicomponent reflection response at the surface and an initial estimate of the multicomponent focusing function. Compared with the scalar version of this approach (Broggini & Snieder 2012; Wapenaar *et al.* 2012, 2014a; Slob *et al.* 2014), the main additional complication is that the focusing functions have a larger overlap with the Green's functions (compare Figs 4c,d with 3b). Whereas in the scalar approach it suffices to define the initial estimate of the focusing function by a single arrival, the initial estimate of the time-reversed multicomponent focusing function $\mathbf{F}_1^+$ should contain all events which overlap with the Green's function $\mathbf{G}^{-,-}$. We have shown with a numerical example that this initial estimate can be obtained from the forward-scattering transmission response, that is, the part of the transmission response which includes direct and forward converted waves but no internal multiples. The modelling of this response requires an estimate of the medium, including the positions of the main interfaces, which are responsible for the wave conversion. In contrast, for the scalar method a smooth version of the medium suffices to define the direct arrival. Note, however, that the requirements for a model that explains forward scattering are less severe than those for a model that explains (backward scattered) internal multiples. In the proposed method, the information for the internal multiples in the retrieved Green's functions comes entirely from the measured reflection response (like in the scalar case). The sensitivity of the methodology towards errors in the initial estimate of the focusing function needs further research. Another issue which needs further investigation is to what extent $\mathbf{F}_1^-$ and the time-reversed coda of $\mathbf{F}_1^+$ are separated in time from the Green's functions. In the considered numerical example they are well separated, but, unlike in the scalar case, in more complex media these functions may extend into the region of the Green's function.

The generalization of the 1-D multicomponent Marchenko scheme (eqs 11–13) to a 3-D scheme goes along similar lines as for the scalar case. The unified 3-D multicomponent Green's function representations (eqs 4 and 5) serve as the starting point. The derivation of the 3-D multicomponent Marchenko scheme requires (i) writing $\mathbf{F}_1^+(\mathbf{x}_0, \mathbf{x}_i', t)$ as the sum of an initial estimate and a coda, analogous to eq. (9), (ii) defining a space-dependent window function (see e.g. Wapenaar *et al.* 2014a), analogous to eq. (10), (iii) applying this window function to both sides of eqs (4) and (5), and (iv) rewriting the resulting Marchenko equations into an iterative scheme for $\mathbf{M}_k^+(\mathbf{x}_0, \mathbf{x}_i', -t)$ and $\mathbf{F}_{1,k+1}^-(\mathbf{x}_0, \mathbf{x}_i', t)$.

Keeping the above-mentioned restrictions in mind, the multicomponent single-sided Marchenko scheme has the potential to retrieve multicomponent Green's functions, which, in turn, can be used for multicomponent imaging, accounting for internal multiples and wave conversion (a preliminary 1-D example is shown in Figs S8–S10).

ACKNOWLEDGEMENTS

We thank Filippo Broggini and an anonymous reviewer for their constructive comments, which helped improve this paper.

REFERENCES

Broggini, F. & Snieder, R., 2012. Connection of scattering principles: a visual and mathematical tour, *Eur. J. Phys.,* **33,** 593–613.

Budreck, D.E. & Rose, J.H., 1990. Three-dimensional inverse scattering in anisotropic elastic media, *Inverse Probl.,* **6,** 331–348.

Campillo, M. & Paul, A., 2003. Long-range correlations in the diffuse seismic coda, *Science,* **299,** 547–549.

Curtis, A., Gerstoft, P., Sato, H., Snieder, R. & Wapenaar, K., 2006. Seismic interferometry: turning noise into signal, *Leading Edge,* **25**(9), 1082–1092.

Da Costa, C., Ravasi, M., Meles, G. & Curtis, A., 2014. Elastic autofocusing via single-sided Marchenko inverse scattering, in SEG, Expanded Abstracts, ST 1.2.

Rose, J.H., 2001. 'Single-sided' focusing of the time-dependent Schrödinger equation, *Phys. Rev. A,* **65,** doi:10.1103/PhysRevA.65.012707.

Rose, J.H., 2002. 'Single-sided' autofocusing of sound in layered materials, *Inverse Probl.,* **18,** 1923–1934.

Schuster, G.T., Yu, J., Sheng, J. & Rickett, J., 2004. Interferometric/daylight seismic imaging, *Geophys. J. Int.,* **157,** 838–852.

Slob, E., Wapenaar, K., Broggini, F. & Snieder, R., 2014. Seismic reflector imaging using internal multiples with Marchenko-type equations, *Geophysics,* **79**(2), S63–S76.

Wapenaar, K., Broggini, F. & Snieder, R., 2012. Creating a virtual source inside a medium from reflection data: heuristic derivation and stationary-phase analysis, *Geophys. J. Int.,* **190,** 1020–1024.

Wapenaar, K., Thorbecke, J., van der Neut, J., Broggini, F., Slob, E. & Snieder, R., 2014a. Green's function retrieval from reflection data, in absence of a receiver at the virtual source position, *J. acoust. Soc. Am.,* **135**(5), 2847–2861.

Wapenaar, K., Thorbecke, J., van der Neut, J., Vasconcelos, I., van Manen, D.-J. & Ravasi, M., 2014b. On the focusing conditions in time-reversed acoustics, seismic interferometry and Marchenko imaging, in SEG, Expanded Abstracts, ST 1.4.

SUPPORTING INFORMATION

Additional Supporting Information may be found in the online version of this article:

Figure S1. Configuration for the reciprocity theorems (eqs A5 and A6).
Figure S2. Directly modelled Green's functions (green) and focusing functions (blue) for oblique incidence ($p = 0.0002\,\mathrm{s\,m^{-1}}$).
Figure S3. Directly modelled Green's functions and focusing functions.
Figure S4. Inverse of the forward-scattering transmission response ($p = 0.0002\,\mathrm{s\,m^{-1}}$). This defines the initial estimate of the focusing functions in Fig. S3.
Figure S5. Reflection response at the surface for oblique incidence ($p = 0.0002\,\mathrm{s\,m^{-1}}$).
Figure S6. Retrieved Green's functions after four iterations of the Marchenko scheme ($p = 0.0002\,\mathrm{s\,m^{-1}}$).
Figure S7. Retrieved Green's functions.
Figure S8. Reflection response at the surface z_0 for a range of rayparameters.
Figure S9. Redatumed reflection response at z_i.
Figure S10. Reflection amplitudes obtained from Fig. S9 (blue marks), compared with the p-dependent reflection coefficients of the interface at $z = 1400$ m. (http://gji.oxfordjournals.org/lookup/suppl/doi:10.1093/gji/ggu313/-/DC1)

Please note: Oxford University Press is not responsible for the content or functionality of any supporting materials supplied by the authors. Any queries (other than missing material) should be directed to the corresponding author for the article.

Geophys. J. Int. (2014) **199**, 001–008

On the Marchenko equation for multicomponent single-sided reflection data: Supporting Information

Kees Wapenaar and Evert Slob
Department of Geoscience and Engineering, Delft University of Technology, P.O. Box 5048, 2600 GA Delft, The Netherlands

27 August 2014

DERIVATION OF THE UNIFIED GREEN'S FUNCTION REPRESENTATION AND FURTHER NUMERICAL EXAMPLES

We define the temporal Fourier transform as

$$u(\mathbf{x},\omega) = \int_{-\infty}^{\infty} u(\mathbf{x},t)\exp(-j\omega t)\mathrm{d}t, \qquad \text{(A1)}$$

where ω is the angular frequency and j is the imaginary unit ($j=\sqrt{-1}$). To keep the notation simple, the same symbol is used for time- and frequency-domain functions. In the frequency domain, equations (1) − (3) become

$$\mathbf{u}^{-}(\mathbf{x}_0,\omega) = \int_{\partial\mathbb{D}_0} \mathbf{R}(\mathbf{x}_0,\mathbf{x}_0',\omega)\mathbf{u}^{+}(\mathbf{x}_0',\omega)\mathrm{d}\mathbf{x}_0', \qquad \text{(A2)}$$

$$\mathbf{u}^{\pm}(\mathbf{x}_i,\omega) = \int_{\partial\mathbb{D}_0} \mathbf{G}^{\pm,+}(\mathbf{x}_i,\mathbf{x}_0',\omega)\mathbf{u}^{+}(\mathbf{x}_0',\omega)\mathrm{d}\mathbf{x}_0' \qquad \text{(A3)}$$

and

$$\mathbf{F}_1^{+}(\mathbf{x}_i,\mathbf{x}_i',\omega) = \mathbf{I}\delta(\mathbf{x}_\mathrm{H}-\mathbf{x}_\mathrm{H}') = \int_{\partial\mathbb{D}_0} \mathbf{T}(\mathbf{x}_i,\mathbf{x}_0'',\omega)\mathbf{F}_1^{+}(\mathbf{x}_0'',\mathbf{x}_i',\omega)\mathrm{d}\mathbf{x}_0'', \qquad \text{(A4)}$$

respectively.

Consider Figure S1, which consists of the two parallel boundaries $\partial\mathbb{D}_0$ and $\partial\mathbb{D}_i$, embedded in the 3D inhomogeneous lossless medium. We consider two states, which will be distinguished by subscripts A and B. Hence, the wave vectors in state A will be denoted by $\mathbf{u}_A^+$ and $\mathbf{u}_A^-$, and those in state B by $\mathbf{u}_B^+$ and $\mathbf{u}_B^-$. Assuming that these wave fields are normalized with respect to the power flux, that the domain between $\partial\mathbb{D}_0$ and $\partial\mathbb{D}_i$ is source-free and the medium parameters in this domain are the same in both states, the wave vectors obey in the space-frequency domain the following reciprocity relations (Wapenaar et al. 2004, 2008)

$$\int_{\partial\mathbb{D}_0} \{(\mathbf{u}_A^+)^t\mathbf{u}_B^- - (\mathbf{u}_A^-)^t\mathbf{u}_B^+\}\mathrm{d}\mathbf{x}_0 = \int_{\partial\mathbb{D}_i} \{(\mathbf{u}_A^+)^t\mathbf{u}_B^- - (\mathbf{u}_A^-)^t\mathbf{u}_B^+\}\mathrm{d}\mathbf{x}_i, \qquad \text{(A5)}$$

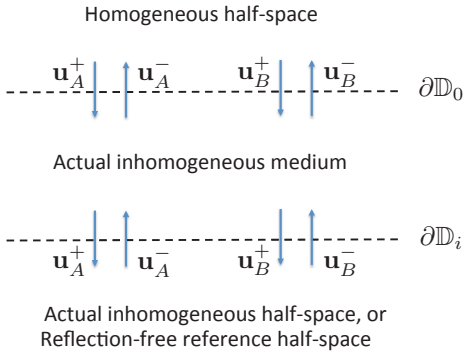

Figure S1. Configuration for the reciprocity theorems (equations (A5) and (A6)).

and

$$\int_{\partial\mathbb{D}_0} \{(\mathbf{u}_A^+)^\dagger\mathbf{u}_B^+ - (\mathbf{u}_A^-)^\dagger\mathbf{u}_B^-\}\mathrm{d}\mathbf{x}_0 = \int_{\partial\mathbb{D}_i} \{(\mathbf{u}_A^+)^\dagger\mathbf{u}_B^+ - (\mathbf{u}_A^-)^\dagger\mathbf{u}_B^-\}\mathrm{d}\mathbf{x}_i, \qquad \text{(A6)}$$

where superscript t denotes transposition and superscript $\dagger$ denotes transposition and complex conjugation. In addition to the assumptions mentioned above, evanescent waves are neglected in equation (A6) at the boundaries $\partial\mathbb{D}_0$ and $\partial\mathbb{D}_i$.

From here onward, we take for state A the fields in the actual medium, which obey equations (A2) and (A3), whereas for state B we take the focusing field in the reference configuration, which obeys equation (A4) (Wapenaar et al. 2014; Slob et al. 2014). Despite the fact that the media are different in these states, reciprocity relations (A5) and (A6) hold for this combination of choices, because the assumption that between $\partial\mathbb{D}_0$ and $\partial\mathbb{D}_i$ the medium parameters are the same in both states is still fulfilled (see Figure 1 in the main paper).

In state A we take for the downgoing wave field at $\partial\mathbb{D}_0$ a spatial delta function times an identity matrix, according to

$$\mathbf{u}_A^+(\mathbf{x}_0,\omega) \rightarrow \mathbf{I}\delta(\mathbf{x}_\mathrm{H}-\mathbf{x}_\mathrm{H}''). \qquad \text{(A7)}$$

Note that we don't write an equal sign because we replace a vector by a matrix. Each column of this matrix represents a unit downgoing wave at $\mathbf{x}_{\mathrm{H}} = \mathbf{x}''_{\mathrm{H}}$ at $\partial\mathbb{D}_0$ for one specific component of the decomposed wave field. According to equation (A2) we obtain for the upgoing field at $\partial\mathbb{D}_0$ in state A

$$\mathbf{u}_A^-(\mathbf{x}_0,\omega) \rightarrow \mathbf{R}(\mathbf{x}_0,\mathbf{x}''_0,\omega). \tag{A8}$$

Similarly, equation (A3) gives the downgoing and upgoing fields at $\partial\mathbb{D}_i$ in state A

$$\mathbf{u}_A^\pm(\mathbf{x}_i,\omega) \rightarrow \mathbf{G}^{\pm,+}(\mathbf{x}_i,\mathbf{x}''_0,\omega). \tag{A9}$$

In state B the downgoing and upgoing fields at $\partial\mathbb{D}_0$ are the incident focusing field and its response, according to

$$\mathbf{u}_B^\pm(\mathbf{x}_0,\omega) \rightarrow \mathbf{F}_1^\pm(\mathbf{x}_0,\mathbf{x}'_i,\omega). \tag{A10}$$

Its response at $\partial\mathbb{D}_i$ is obtained from equation (A4), i.e.

$$\mathbf{u}_B^+(\mathbf{x}_i,\omega) \rightarrow \mathbf{I}\delta(\mathbf{x}_{\mathrm{H}} - \mathbf{x}'_{\mathrm{H}}). \tag{A11}$$

Because the reference configuration is reflection-free below $\partial\mathbb{D}_i$ there is no upgoing field at $\partial\mathbb{D}_i$, hence

$$\mathbf{u}_B^-(\mathbf{x}_i,\omega) \rightarrow \mathbf{O}. \tag{A12}$$

Substituting equations (A7) – (A12) into equations (A5) and (A6), using $\{\mathbf{R}(\mathbf{x}_0,\mathbf{x}''_0,\omega)\}^t = \mathbf{R}(\mathbf{x}''_0,\mathbf{x}_0,\omega)$, $\{\mathbf{G}^{-,+}(\mathbf{x}'_i,\mathbf{x}''_0,\omega)\}^t = \mathbf{G}^{-,+}(\mathbf{x}''_0,\mathbf{x}'_i,\omega)$ and $\{\mathbf{G}^{+,+}(\mathbf{x}'_i,\mathbf{x}''_0,\omega)\}^t = -\mathbf{G}^{-,-}(\mathbf{x}''_0,\mathbf{x}'_i,\omega)$ (Wapenaar 1996), gives

$$\mathbf{G}^{-,+}(\mathbf{x}''_0,\mathbf{x}'_i,\omega) + \mathbf{F}_1^-(\mathbf{x}''_0,\mathbf{x}'_i,\omega) = \int_{\partial\mathbb{D}_0} \mathbf{R}(\mathbf{x}''_0,\mathbf{x}_0,\omega)\mathbf{F}_1^+(\mathbf{x}_0,\mathbf{x}'_i,\omega)\mathrm{d}\mathbf{x}_0 \tag{A13}$$

and

$$\mathbf{G}^{-,-}(\mathbf{x}''_0,\mathbf{x}'_i,\omega) + \{\mathbf{F}_1^+(\mathbf{x}''_0,\mathbf{x}'_i,\omega)\}^* = \int_{\partial\mathbb{D}_0} \mathbf{R}(\mathbf{x}''_0,\mathbf{x}_0,\omega)\{\mathbf{F}_1^-(\mathbf{x}_0,\mathbf{x}'_i,\omega)\}^*\mathrm{d}\mathbf{x}_0, \tag{A14}$$

respectively. Here superscript $*$ denotes complex conjugation. In the time domain, these equations read

$$\mathbf{G}^{-,+}(\mathbf{x}''_0,\mathbf{x}'_i,t) + \mathbf{F}_1^-(\mathbf{x}''_0,\mathbf{x}'_i,t) = \int_{\partial\mathbb{D}_0} \mathrm{d}\mathbf{x}_0 \int_{-\infty}^{t} \mathbf{R}(\mathbf{x}''_0,\mathbf{x}_0,t-t')\mathbf{F}_1^+(\mathbf{x}_0,\mathbf{x}'_i,t')\mathrm{d}t' \tag{A15}$$

and

$$\mathbf{G}^{-,-}(\mathbf{x}''_0,\mathbf{x}'_i,t) + \mathbf{F}_1^+(\mathbf{x}''_0,\mathbf{x}'_i,-t) = \int_{\partial\mathbb{D}_0} \mathrm{d}\mathbf{x}_0 \int_{-\infty}^{t} \mathbf{R}(\mathbf{x}''_0,\mathbf{x}_0,t-t')\mathbf{F}_1^-(\mathbf{x}_0,\mathbf{x}'_i,-t')\mathrm{d}t', \tag{A16}$$

respectively.

From here onward we consider a horizontally layered medium and wave propagation in the (x,z)-plane only. We define the spatial Fourier transform as

$$u(p,z,\omega) = \int_{-\infty}^{\infty} u(x,z,\omega)\exp(j\omega px)\mathrm{d}x, \tag{A17}$$

where p is the horizontal rayparameter. In the rayparameter-frequency domain, equations (A2) – (A6) become

$$\mathbf{u}^-(p,z_0,\omega) = \mathbf{R}(p,z_0,\omega)\mathbf{u}^+(p,z_0,\omega), \tag{A18}$$

$$\mathbf{u}^\pm(p,z_i,\omega) = \mathbf{G}^{\pm,+}(p,z_i,z_0,\omega)\mathbf{u}^+(p,z_0,\omega), \tag{A19}$$

$$\mathbf{F}_1^+(p,z_i,z_i,\omega) = \mathbf{I} = \mathbf{T}(p,z_i,z_0,\omega)\mathbf{F}_1^+(p,z_0,z_i,\omega), \tag{A20}$$

$$\{\mathbf{u}_A^+(-p,z_0,\omega)\}^t\mathbf{u}_B^-(p,z_0,\omega) - \{\mathbf{u}_A^-(-p,z_0,\omega)\}^t\mathbf{u}_B^+(p,z_0,\omega) = \{\mathbf{u}_A^+(-p,z_i,\omega)\}^t\mathbf{u}_B^-(p,z_i,\omega) - \{\mathbf{u}_A^-(-p,z_i,\omega)\}^t\mathbf{u}_B^+(p,z_i,\omega) \tag{A21}$$

and

$$\{\mathbf{u}_A^+(p,z_0,\omega)\}^\dagger\mathbf{u}_B^+(p,z_0,\omega) - \{\mathbf{u}_A^-(p,z_0,\omega)\}^\dagger\mathbf{u}_B^-(p,z_0,\omega) = \{\mathbf{u}_A^+(p,z_i,\omega)\}^\dagger\mathbf{u}_B^+(p,z_i,\omega) - \{\mathbf{u}_A^-(p,z_i,\omega)\}^\dagger\mathbf{u}_B^-(p,z_i,\omega), \tag{A22}$$

respectively. Note that equation (A22) only holds for non-evanescent fields at z_0 and z_i. Analogous to equations (A7) – (A12) we make the following replacements

$$\begin{aligned}
\mathbf{u}_A^+(p,z_0,\omega) &\rightarrow \mathbf{I}, && \text{(A23)}\\
\mathbf{u}_A^-(p,z_0,\omega) &\rightarrow \mathbf{R}(p,z_0,\omega) = \{\mathbf{R}(-p,z_0,\omega)\}^t, && \text{(A24)}\\
\mathbf{u}_A^\pm(p,z_i,\omega) &\rightarrow \mathbf{G}^{\pm,+}(p,z_i,z_0,\omega) && \\
&\quad = \mp\{\mathbf{G}^{-,\mp}(-p,z_0,z_i,\omega)\}^t, && \text{(A25)}\\
\mathbf{u}_B^\pm(p,z_0,\omega) &\rightarrow \mathbf{F}_1^\pm(p,z_0,z_i,\omega), && \text{(A26)}\\
\mathbf{u}_B^+(p,z_i,\omega) &\rightarrow \mathbf{I}, && \text{(A27)}\\
\mathbf{u}_B^-(p,z_i,\omega) &\rightarrow \mathbf{O}. && \text{(A28)}
\end{aligned}$$

Substitution into equations (A21) and (A22) gives

$$\mathbf{G}^{-,+}(p,z_0,z_i,\omega) + \mathbf{F}_1^-(p,z_0,z_i,\omega) = \mathbf{R}(p,z_0,\omega)\mathbf{F}_1^+(p,z_0,z_i,\omega) \tag{A29}$$

and

$$\mathbf{G}^{-,-}(-p,z_0,z_i,\omega) + \{\mathbf{F}_1^+(p,z_0,z_i,\omega)\}^* = \mathbf{R}(-p,z_0,\omega)\{\mathbf{F}_1^-(p,z_0,z_i,\omega)\}^*, \tag{A30}$$

respectively. In the rayparameter intercept-time domain (Stoffa 1989) these expressions become

$$\mathbf{G}^{-,+}(p,z_0,z_i,\tau) + \mathbf{F}_1^-(p,z_0,z_i,\tau) = \int_{-\infty}^{\tau} \mathbf{R}(p,z_0,\tau-\tau')\mathbf{F}_1^+(p,z_0,z_i,\tau')\mathrm{d}\tau' \tag{A31}$$

and (replacing p by $-p$)

$$\mathbf{G}^{-,-}(p,z_0,z_i,\tau) + \mathbf{F}_1^+(-p,z_0,z_i,-\tau) = \int_{-\infty}^{\tau} \mathbf{R}(p,z_0,\tau-\tau')\mathbf{F}_1^-(-p,z_0,z_i,-\tau')\mathrm{d}\tau', \tag{A32}$$

respectively.

For the model of Figure 2 in the main paper, with $z_0 = 0$m and $z_i = 1000$m, the elements of the directly modeled elastodynamic Green's functions $\mathbf{G}^{-,\pm}(p,z_0,z_i,\tau)$ and focusing functions $\mathbf{F}_1^\pm(\mp p,z_0,z_i,\mp\tau)$ are shown in Figures S2 and S3. Figure S4 shows the elements of the inverse of the forward-scattering transmission response, $\mathbf{T}_{\mathrm{fs}}^{\mathrm{inv}}(-p,z_i,z_0,-\tau)$. The latter, together with the reflection response $\mathbf{R}(p,z_0,\tau)$ (Figure S5), forms the input of the multicomponent single-sided Marchenko scheme of equations (11) – (13) in the main paper. The retrieved Green's functions $\mathbf{G}^{-,\pm}(p,z_0,z_i,\tau)$ after four iterations, are shown in Figures S6 and S7.

(Text continues on page 5).

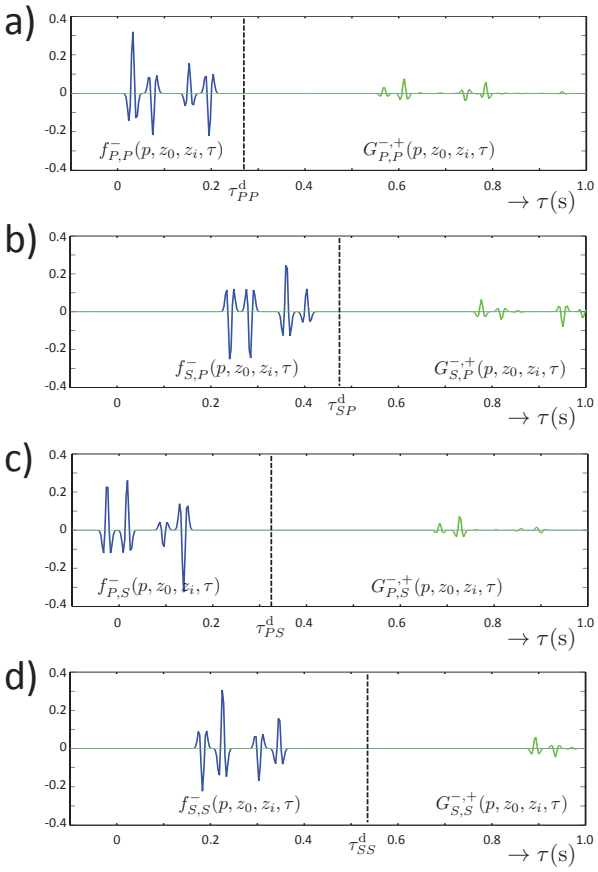

Figure S2. Directly modeled Green's functions (green) and focusing functions (blue) for oblique incidence ($p = 0.0002$ s/m).

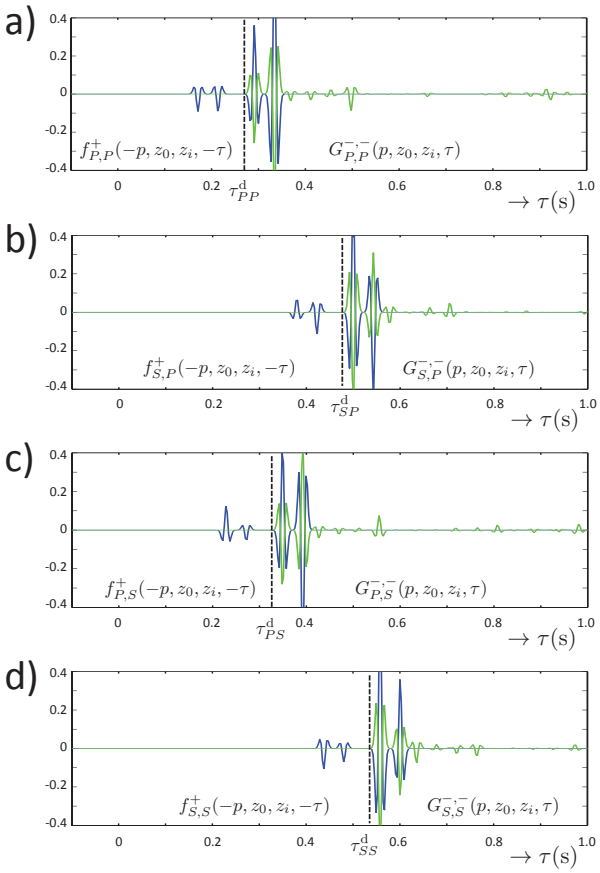

Figure S3. Directly modeled Green's functions and focusing functions (continued).

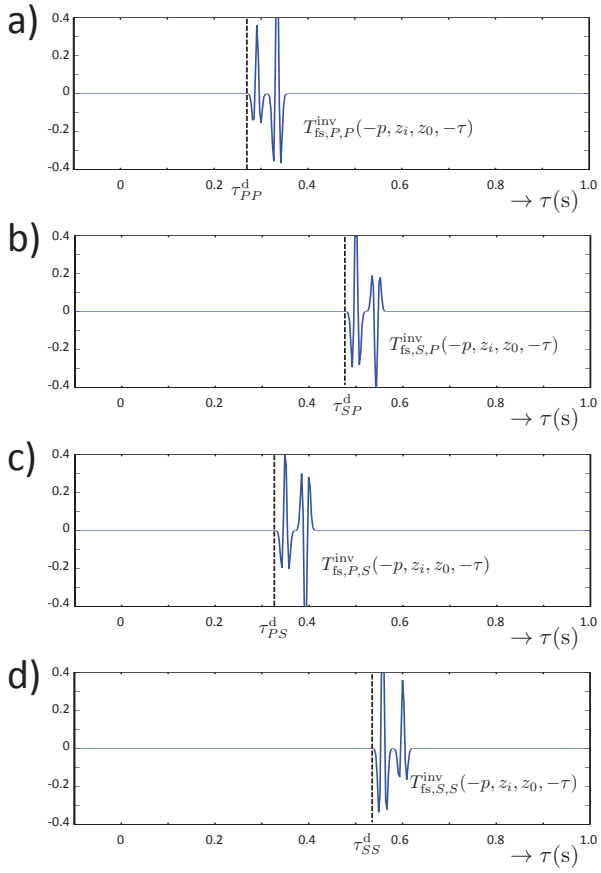

Figure S4. Inverse of the forward-scattering transmission response ($p = 0.0002$ s/m). This defines the initial estimate of the focusing functions in Figure S3.

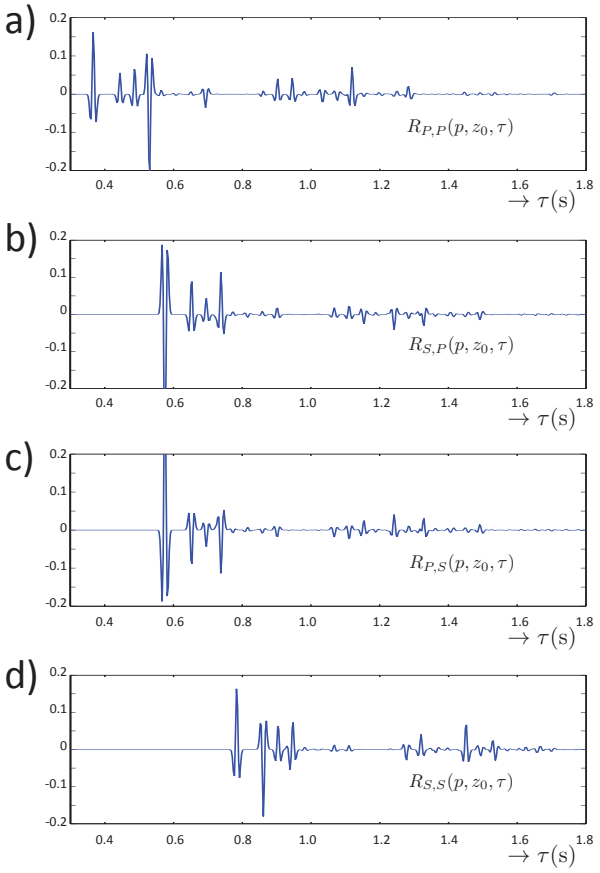

Figure S5. Reflection response at the surface for oblique incidence ($p = 0.0002$ s/m).

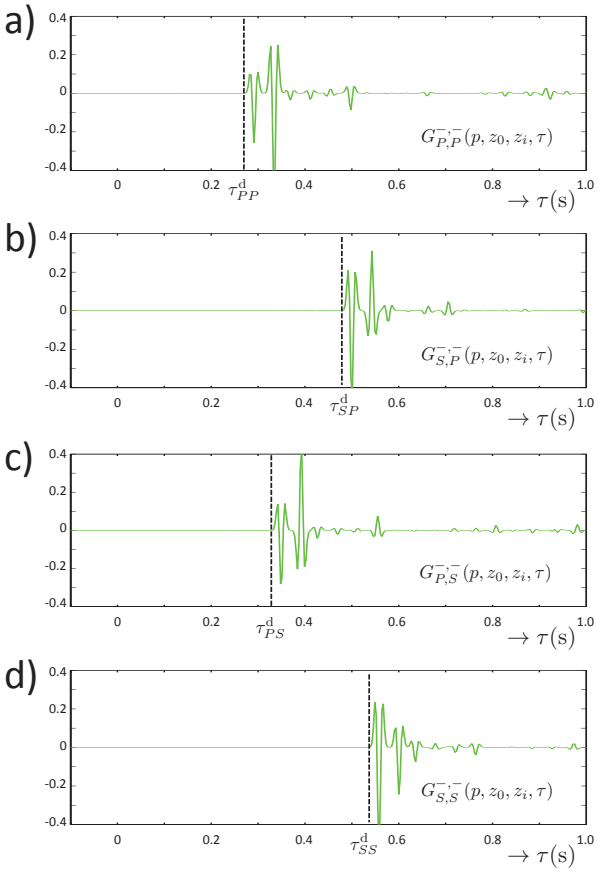

Figure S6. Retrieved Green's functions after four iterations of the Marchenko scheme ($p = 0.0002$ s/m).

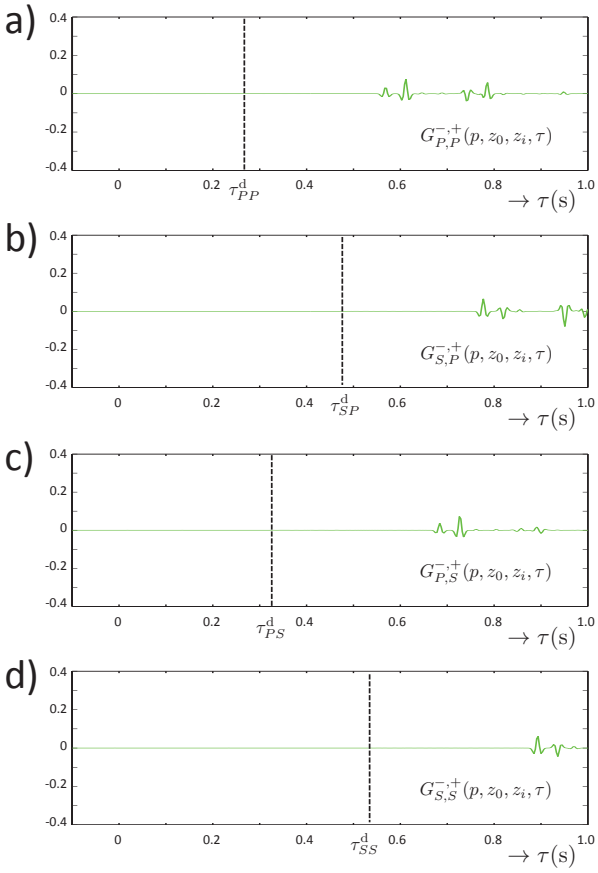

Figure S7. Retrieved Green's functions (continued).

The reciprocals of the retrieved Green's functions, i.e.,

$$\mathbf{G}^{+,+}(p,z_i,z_0,\tau) = -\{\mathbf{G}^{-,-}(-p,z_0,z_i,\tau)\}^t, \qquad \text{(A33)}$$

$$\mathbf{G}^{-,+}(p,z_i,z_0,\tau) = +\{\mathbf{G}^{-,+}(-p,z_0,z_i,\tau)\}^t, \qquad \text{(A34)}$$

(see equation A25) are mutually related via the reflection response at z_i, according to

$$\mathbf{G}^{-,+}(p,z_i,z_0,\tau) = \int_{-\infty}^{\tau} \mathbf{R}(p,z_i,\tau-\tau')\mathbf{G}^{+,+}(p,z_i,z_0,\tau')\mathrm{d}\tau' \qquad \text{(A35)}$$

(Riley & Claerbout 1976; Wapenaar et al. 2000; Amundsen 2001). This expression states that the downgoing field $\mathbf{G}^{+,+}$ at z_i, convolved with the reflection response $\mathbf{R}$ at z_i, gives the upgoing field $\mathbf{G}^{-,+}$ at z_i. Note that $\mathbf{G}^{+,+}$ and $\mathbf{G}^{-,+}$ are defined in the actual medium, whereas $\mathbf{R}(p,z_i,\tau)$ is defined in a reference medium that is identical to the actual medium below z_i and reflection-free above z_i. Resolving $\mathbf{R}$ from equation (A35) involves "seismic interferometry by deconvolution" (Snieder 2006; Vasconcelos & Snieder 2008; van der Neut et al. 2011). We illustrate this with a numerical example. Figure S8 shows again the elements of the reflection response $\mathbf{R}(p,z_0,\tau)$ at the surface, this time for a range of p-values (the last trace in each panel corresponds with Figure S5). Similar as above, the Green's functions for all p-values are retrieved via the Marchenko scheme. Next, the reflection response at z_i, $\mathbf{R}(p,z_i,\tau)$, is resolved from these Green's functions by inverting equation (A35) for each p-value. This "redatumed" reflection response is shown in Figure S9. This figure clearly shows the response of the single reflector below z_i (the interface at $z = 1400$ m, see Figure 2 in the main paper). The p-dependent reflection amplitudes are retrieved from these reflection responses after envelope detection. They are denoted by the blue marks in Figure S10. The green curves in this figure are the modeled p-dependent reflection coefficients of the interface at $z = 1400$ m. Note that for this idealized example the match is perfect.

(Text continues on page 7).

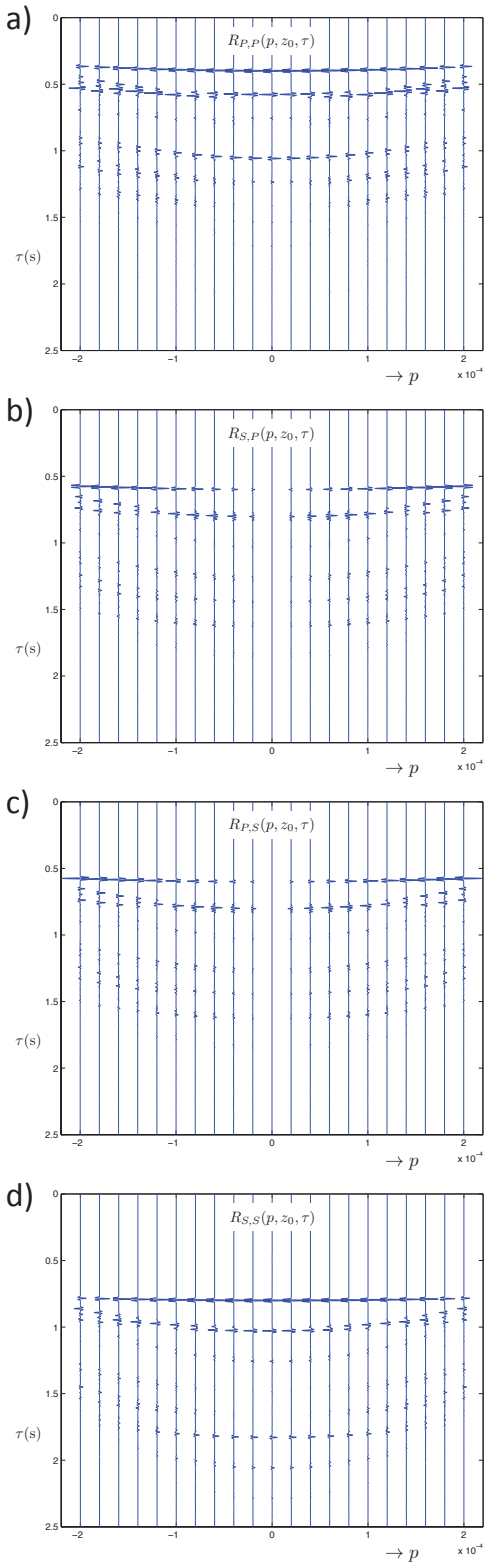

Figure S8. Reflection response at the surface z_0 for a range of rayparameters.

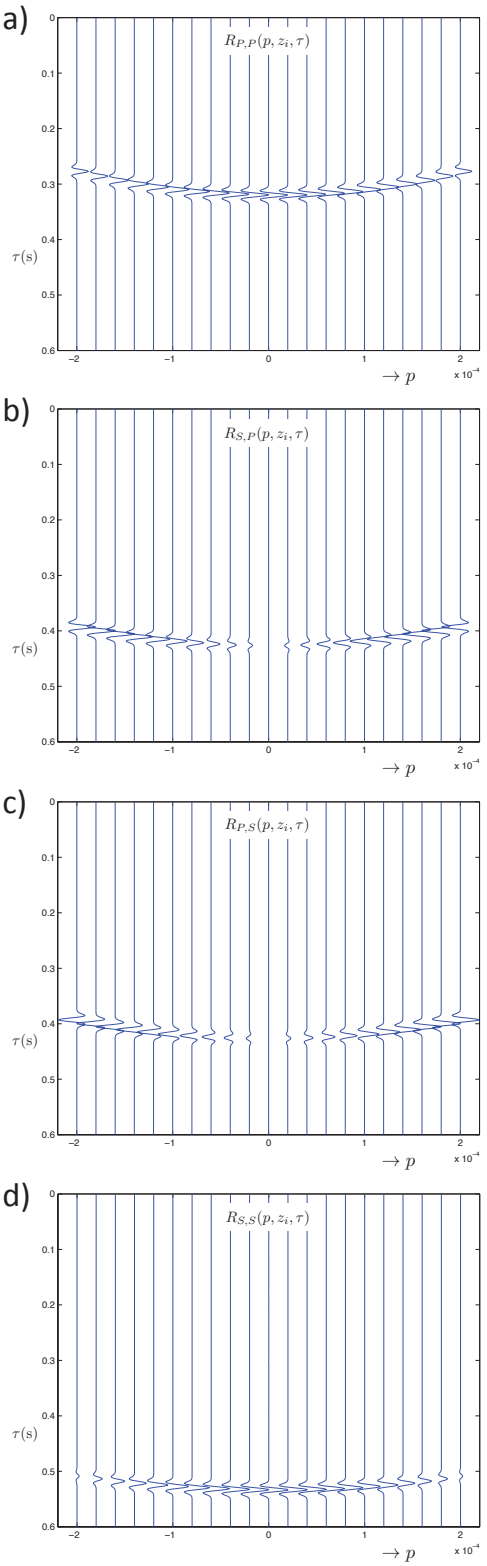

Figure S9. Redatumed reflection response at z_i.

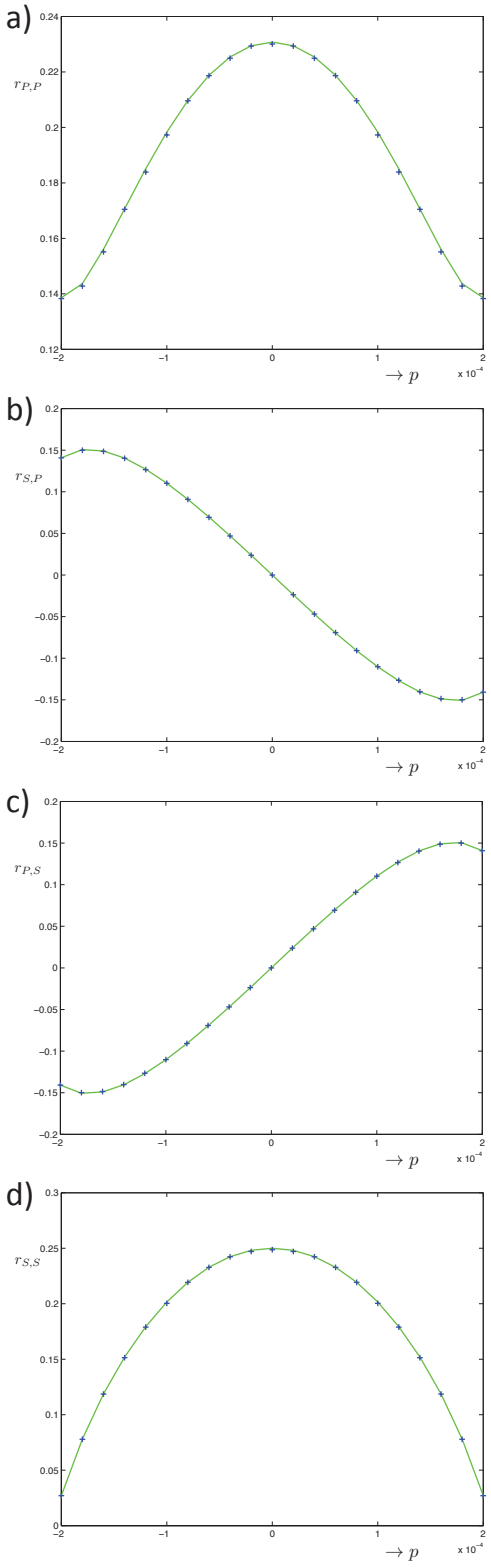

Figure S10. Reflection amplitudes obtained from Figure S9 (blue marks), compared with the p-dependent reflection coefficients of the interface at $z = 1400$ m.

Finally we discuss how the decomposed wave fields and Green's functions are related to measurable field quantities and the standard Green's functions encountered in seismological textbooks.

For elastodynamic wave fields in the (x, z)-plane in a horizontally layered medium we relate the measurable (two-way) wave field vector $\mathbf{q}(p, z, \omega)$ to the decomposed (one-way) wave field vector $\mathbf{u}(p, z, \omega)$ via a composition matrix $\mathbf{L}(p, z)$, according to

$$\mathbf{q}(p, z, \omega) = \mathbf{L}(p, z)\mathbf{u}(p, z, \omega), \tag{A36}$$

with

$$\mathbf{q}(p, z, \omega) = \begin{pmatrix} -\boldsymbol{\tau} \\ \mathbf{v} \end{pmatrix}(p, z, \omega), \tag{A37}$$

where $\boldsymbol{\tau}$ is the traction and $\mathbf{v}$ the particle velocity, and

$$\mathbf{u}(p, z, \omega) = \begin{pmatrix} \mathbf{u}^+ \\ \mathbf{u}^- \end{pmatrix}(p, z, \omega), \tag{A38}$$

where $\mathbf{u}^+$ and $\mathbf{u}^-$ are the flux-normalized decomposed downgoing and upgoing wave fields. The flux-normalized composition matrix $\mathbf{L}(p, z)$ is defined as (Frasier 1970; Ursin 1983; Wapenaar et al. 2008)

$$\mathbf{L}(p, z) = \begin{pmatrix} \mathbf{L}_1^+ & \mathbf{L}_1^- \\ \mathbf{L}_2^+ & \mathbf{L}_2^- \end{pmatrix}(p, z), \tag{A39}$$

where

$$\mathbf{L}_1^{\pm}(p, z) = c_S^2 \left(\frac{\rho}{2}\right)^{\frac{1}{2}} \begin{pmatrix} \pm 2pq_P^{\frac{1}{2}} & -(c_S^{-2} - 2p^2)/q_S^{\frac{1}{2}} \\ (c_S^{-2} - 2p^2)/q_P^{\frac{1}{2}} & \pm 2pq_S^{\frac{1}{2}} \end{pmatrix}, \tag{A40}$$

$$\mathbf{L}_2^{\pm}(p, z) = (2\rho)^{-\frac{1}{2}} \begin{pmatrix} p/q_P^{\frac{1}{2}} & \mp q_S^{\frac{1}{2}} \\ \pm q_P^{\frac{1}{2}} & p/q_S^{\frac{1}{2}} \end{pmatrix}, \tag{A41}$$

with $\rho(z)$ the mass density and $c_S(z)$ the S-wave velocity. The vertical P- and S-wave slownesses $q_P(p, z)$ and $q_S(p, z)$, respectively, are defined as

$$q_P(p, z) = (c_P^{-2}(z) - p^2)^{\frac{1}{2}}, \tag{A42}$$

$$q_S(p, z) = (c_S^{-2}(z) - p^2)^{\frac{1}{2}}, \tag{A43}$$

with $c_P(z)$ the P-wave velocity. Because of the flux-normalization, composition matrix $\mathbf{L}(p, z)$ has a simple inverse. The decomposition matrix $\mathbf{L}^{-1}(p, z)$ is given by

$$\mathbf{L}^{-1}(p, z) = -\mathbf{N}^{-1}\mathbf{L}^t(-p, z)\mathbf{N}, \tag{A44}$$

with

$$\mathbf{N} = \begin{pmatrix} \mathbf{O} & \mathbf{I} \\ -\mathbf{I} & \mathbf{O} \end{pmatrix}, \tag{A45}$$

hence

$$\mathbf{L}^{-1}(p, z) = \begin{pmatrix} -\{\mathbf{L}_2^-\}^t & \{\mathbf{L}_1^-\}^t \\ \{\mathbf{L}_2^+\}^t & -\{\mathbf{L}_1^+\}^t \end{pmatrix}(-p, z). \tag{A46}$$

We group the Green's matrices for the decomposed wave fields into a single one-way Green's matrix $\mathbf{G}_I(p, z_0, z_i, \omega)$, according to

$$\mathbf{G}_I(p, z_0, z_i, \omega) = \begin{pmatrix} \mathbf{G}^{+,+} & \mathbf{G}^{+,-} \\ \mathbf{G}^{-,+} & \mathbf{G}^{-,-} \end{pmatrix} (p, z_0, z_i, \omega). \quad \text{(A47)}$$

We define the two-way Green's matrix $\mathbf{G}_{II}(p, z_0, z_i, \omega)$ as follows

$$\mathbf{G}_{II}(p, z_0, z_i, \omega) = \begin{pmatrix} \mathbf{G}^{\tau,f} & \mathbf{G}^{\tau,h} \\ \mathbf{G}^{v,f} & \mathbf{G}^{v,h} \end{pmatrix} (p, z_0, z_i, \omega). \quad \text{(A48)}$$

Here the first superscripts (τ and v) refer to the observed wave field at z_0 (traction and particle velocity, respectively), whereas the second superscripts (f and h) refer to the source type at z_i (force and deformation, respectively). Note that the lower left matrix $\mathbf{G}^{v,f}(p, z_0, z_i, \omega)$ is the common Green's tensor in terms of particle velocity components in response to force sources. The two-way Green's matrix is related to the one-way Green's matrix according to

$$\mathbf{G}_{II}(p, z_0, z_i, \omega) = \mathbf{L}(p, z_0)\mathbf{G}_I(p, z_0, z_i, \omega)\mathbf{L}^{-1}(p, z_i), \quad \text{(A49)}$$

or, using equation (A44),

$$\mathbf{G}_{II}(p, z_0, z_i, \omega) = -\mathbf{L}(p, z_0)\mathbf{G}_I(p, z_0, z_i, \omega)\mathbf{N}^{-1}\mathbf{L}^t(-p, z_i)\mathbf{N}. \quad \text{(A50)}$$

Similarly, for the unified Green's matrices in 3D inhomogeneous media we write

$$\mathbf{G}_{II}(\mathbf{x}_0'', \mathbf{x}_i', \omega) = -\boldsymbol{\mathcal{L}}(z_0, \omega)\mathbf{G}_I(\mathbf{x}_0'', \mathbf{x}_i', \omega)\mathbf{N}^{-1}\underleftarrow{\boldsymbol{\mathcal{L}}}^t(z_i, \omega)\mathbf{N}, \quad \text{(A51)}$$

where composition matrix $\boldsymbol{\mathcal{L}}(z_0, \omega)$ contains the appropriate pseudo-differential operators (Fishman et al. 1987; Corones et al. 1983, 1992; Fishman 1993; Haines & de Hoop 1996; de Hoop 1996; Wapenaar & Grimbergen 1996; Wapenaar et al. 2008), and where $\underleftarrow{\boldsymbol{\mathcal{L}}}^t(z_i, \omega)$ is the transposed composition matrix, with the pseudo-differential operators acting on the quantities left of it.

REFERENCES

Amundsen, L., 2001. Elimination of free-surface related multiples without need of the source wavelet, *Geophysics*, **66**(1), 327–341.

Corones, J. P., Davison, M. E., & Krueger, R. J., 1983. Direct and inverse scattering in the time domain via invariant imbedding equations, *Journal of the Acoustical Society of America*, **74**, 1535–1541.

Corones, J. P., Kristensson, G., Nelson, P., & Seth, D., 1992. *Invariant imbedding and inverse problems*, SIAM, Philadelphia.

de Hoop, M. V., 1996. Generalization of the Bremmer coupling series, *J. Math. Phys.*, **37**, 3246–3282.

Fishman, L., 1993. One-way propagation methods in direct and inverse scalar wave propagation modeling, *Radio Science*, **28**(5), 865–876.

Fishman, L., McCoy, J. J., & Wales, S. C., 1987. Factorization and path integration of the Helmholtz equation: Numerical algorithms, *Journal of the Acoustical Society of America*, **81**(5), 1355–1376.

Frasier, C. W., 1970. Discrete time solution of plane P-SV waves in a plane layered medium, *Geophysics*, **35**, 197–219.

Haines, A. J. & de Hoop, M. V., 1996. An invariant imbedding analysis of general wave scattering problems, *J. Math. Phys.*, **37**, 3854–3881.

Riley, D. C. & Claerbout, J. F., 1976. 2-D multiple reflections, *Geophysics*, **41**, 592–620.

Slob, E., Wapenaar, K., Broggini, F., & Snieder, R., 2014. Seismic reflector imaging using internal multiples with Marchenko-type equations, *Geophysics*, **79**(2), S63–S76.

Snieder, R., 2006. Retrieving the Green's function of the diffusion equation from the response to a random forcing, *Physical Review E*, **74**, 046620.

Stoffa, P. L., 1989. *Tau-p - A plane wave approach to the analysis of seismic data*, Kluwer Academic Publishers, Dordrecht.

Ursin, B., 1983. Review of elastic and electromagnetic wave propagation in horizontally layered media, *Geophysics*, **48**, 1063–1081.

van der Neut, J., Thorbecke, J., Mehta, K., Slob, E., & Wapenaar, K., 2011. Controlled-source interferometric redatuming by crosscorrelation and multidimensional deconvolution in elastic media, *Geophysics*, **76**(4), SA63–SA76.

Vasconcelos, I. & Snieder, R., 2008. Interferometry by deconvolution: Part 2 - Theory for elastic waves and application to drill-bit seismic imaging, *Geophysics*, **73**(3), S129–S141.

Wapenaar, C. P. A., 1996. One-way representations of seismic data, *Geophysical Journal International*, **127**, 178–188.

Wapenaar, C. P. A. & Grimbergen, J. L. T., 1996. Reciprocity theorems for one-way wave fields, *Geophysical Journal International*, **127**, 169–177.

Wapenaar, K., Fokkema, J., Dillen, M., & Scherpenhuijsen, P., 2000. One-way acoustic reciprocity and its applications in multiple elimination and time-lapse seismics, in *SEG, Expanded Abstracts*, pp. 2377–2380.

Wapenaar, K., Thorbecke, J., & Draganov, D., 2004. Relations between reflection and transmission responses of three-dimensional inhomogeneous media, *Geophysical Journal International*, **156**, 179–194.

Wapenaar, K., Slob, E., & Snieder, R., 2008. Seismic and electromagnetic controlled-source interferometry in dissipative media, *Geophysical Prospecting*, **56**, 419–434.

Wapenaar, K., Thorbecke, J., van der Neut, J., Broggini, F., Slob, E., & Snieder, R., 2014. Green's function retrieval from reflection data, in absence of a receiver at the virtual source position, *Journal of the Acoustical Society of America*, **135**(5), 2847–2861.